IEEE Access
Multidisciplinary | Rapid Review | Open Access Journal

Received April 12, 2020, accepted April 17, 2020, date of publication April 24, 2020, date of current version May 11, 2020.

Digital Object Identifier 10.1109/ACCESS.2020.2990160

A Modeling Study of the Impact of the Sea Surface Temperature on the Backscattering Coefficient and Wind Field Retrieval

YIHUAN PENG[1], XUETONG XIE[1], MINGSEN LIN[2], (Member, IEEE), CUIHONG PAN[1], AND HAITAO LI[1]

[1]School of Geographical Sciences, Guangzhou University, Guangzhou 510006, China
[2]National Satellite Ocean Application Service, Beijing 100081, China

Corresponding author: Xuetong Xie (xtxie2013@163.com)

This work was supported in part by the National Natural Science Foundation of China under Grant 41876204 and Grant 41476152, and in part by the National Key Research and Development Project of China under Grant 2016YFC1401001.

ABSTRACT The sea surface temperature (SST) actively impacts the backscattering coefficient measured by scatterometers and the wind retrieval accuracy. However, none of the geophysical model functions (GMFs) currently used in operational wind retrieval considers the effect of the SST. With the HY-2A scatterometer as the research subject, this paper attempts to quantitatively analyze the effect of the SST on the backscattering coefficient for the first time and establish a new GMF by the Fourier series method (containing only cosine terms), which adopts the SST as the independent variable. The collocated Level 2A radar backscatter measurement data of the HY-2A scatterometer and the European Centre for Medium-Range Weather Forecasts (ECMWF) reanalysis wind data are used to build the new SST-dependent GMF that considers the influence of the SST in the model. The study indicates that the SST effects are wind speed dependent and more significant under vertical-vertical (VV) polarization. The backscattering coefficient increases with increasing SST in the wind speed range of 5-15 m/s. In addition, with increasing wind speed, the influence of the SST gradually decreases. Finally, the new GMF was applied to retrieve the ocean surface wind, which was compared to the conventional GMF to validate its performance. The experimental results indicate that the accuracy of wind field retrieval by the new GMF is considerably improved and the systematic deviation in the wind speed is effectively corrected. This study potentially contributes to a better understanding of the microwave backscattering behavior of the ocean surface and provides a way to further improve the wind retrieval accuracy of the HY-2A scatterometer as well as of other Ku-band scatterometers.

INDEX TERMS Fourier series, geophysical model function (GMF), wind field retrieval, SST.

I. INTRODUCTION

Remote sensing technology has developed rapidly in recent decades. Data processing and information extraction are the core content of the remote sensing application technology system. Among them, Earth surface parameter retrieval and remote sensing image classification are research areas of increased interest in the field of remote sensing applications. In recent years, domestic and foreign scholars have introduced many new technologies and proposed many innovative models and algorithms for different application fields and application scenarios, which have effectively promoted the progress of remote sensing technology and greatly improved remote sensing applications [1]–[7]. Sea surface wind field remote sensing is an important branch of remote sensing applications that has been widely applied in both civil and military applications [8]–[10] and has gradually become one of the current remote sensing research hotspots. Moreover, the emergence of microwave scatterometers provides new technical support for humans to obtain global sea surface wind field information at a higher spatiotemporal resolution. Therefore, obtaining sea surface wind field data at high spatial and temporal resolutions has a very important scientific research value and practical significance. In the study of sea surface wind field retrieval, domestic and foreign scholars have intensively investigated the relationship

The associate editor coordinating the review of this manuscript and approving it for publication was Lefei Zhang.

between microwave backscatter data and wind field and have proposed many geophysical model functions (GMFs) for wind field inversion, such as the GMFs for the C-band, including CMOD4, CMOD5/COMD5N and CMOD7, and those for the Ku-band, including NSCAT-II, Qscat-1, and Ku-2011 [11]–[19].

A GMF is a quantitative model that is based on the relationships between the backscattering coefficient, radar measurement parameters, and environmental parameters, such as the wind speed and direction. Thus far, because the relationship between wind vectors and ocean surface geometry and the interaction mechanism between electromagnetic waves and sea surface have not been thoroughly understood, it is difficult to establish a strict theoretical model [18]. Generally, a GMF is a prerequisite for the inversion of the wind field by scatterometer data. To improve the quality of wind field inversion, the parameters selected for establishing the GMF are particularly critical. To date, the GMFs used for operational wind retrieval have only considered the main factors, such as the radar wavelength, polarization, incident angle, wind speed, wind direction, and radar observing azimuth, while ignoring the influence of the sea surface temperature (SST). The reasons can be summarized as follows. On the one hand, the interaction mechanism between the SST and backscattering coefficient has not been clearly explained. On the other hand, insufficient stable and reliable data are available for empirical modeling, so a GMF containing the SST as a factor has not been built for operational wind retrieval.

However, scholars have remained interested in the influence of the SST on backscattering and wind retrieval since the 1980s. Studies have found that the difference between the wind speeds retrieved by scatterometers and those measured by buoys is strongly correlated with the SST [19], and the SST may affect capillary waves and backscattering through the viscosity [20]–[22]. Generally, scatterometer radar backscattering depends on the relationship between the surface stress and surface roughness. Grodsky proposed that the SST can alter the growth rate of centimeter-scale waves through its impact on the air and water densities and water viscosity, and he found that the effects of the SST on Ku-band GMFs are much larger than those on C-band GMFs [21]. In addition, Xie *et al.* established the first GMF containing the SST by the neural network algorithm in China, and Wang recently improved the Ku-band GMF called NSCAT-5, which considers the effects of the SST on the wind data retrieved by RapidScat; both research groups found that the backscattering coefficient changes regularly with the SST under certain conditions [23], [24]. Therefore, it is necessary to consider the SST in the GMF, but expanding the model parameters for wind field retrieval causes new problems. Xie *et al.* [23] found that the amount of experimental data after spatiotemporal matching and preprocessing was not sufficient, especially when the temperature factor was treated as an independent variable. The smaller amount of data additionally intensifies the effect of scatterometer measurement noise in modeling, so the experimental results still need to be further verified. Therefore, the expansion of the GMF to include the influence of the SST is the main problem to be solved in this paper.

From another perspective, China has attained remarkable progress in marine satellites since 2002 and has established a marine satellite system including water color satellites, dynamic environment satellites, and surveillance satellites. The HY-2 series satellites are mainly used for ocean dynamic environment detection, which can simultaneously obtain the global ocean surface wind field, SST, sea surface height and other marine dynamic environmental parameters. At present, the HY-2 series satellites comprise two satellites: HY-2A and HY-2B. They operate steadily and measure global ocean surface winds. The measurement accuracy of each parameter is better than the design requirements [25], [26]. Against this background, this study carries out research for the first time on building a GMF containing the SST factor (GMFCT) and the corresponding wind field retrieval algorithm for the HY-2A satellite scatterometer to further improve the measurement accuracy of the sea surface wind field and to enhance the application level of the HY-2 series satellites, thereby enhancing their utility in oceanographic and meteorological research and other applications.

In summary, the existing GMFs have limitations, which is the main cause of wind retrieval errors and the main obstacle to the further improvement of the inversion precision. At the same time, driven by the application demand, researchers urgently need to build a GMF with a higher precision. Including the SST in the GMF is one possible way to improve the model accuracy and to better understand the behavior of radar microwave backscattering from the sea surface. Therefore, according to the characteristics of the HY-2A scatterometer and the limitations of previous studies, this paper builds a GMFCT for the HY-2A scatterometer by the Fourier series method (containing only cosine terms). The reason for selecting the partial Fourier series containing only cosine terms is that the backscattering coefficient is an even function of the relative wind direction. Theoretically, the higher the order of the Fourier series expansion is, the more accurate the model is. In previous research, it has proved sufficient to use the first three terms of the Fourier series to build a GMF without including the SST factor. However, when the SST is considered the independent variable in modeling, the third-order Fourier series approximation is no longer accurate enough for fitting the GMF containing the SST factor. Thus, this study uses the fifth-order Fourier series expansion to build the GMFCT, which can better include the impact of the SST. The impact laws of the SST on the backscattering coefficient of the HY-2A scatterometer can be characterized by the GMFCT. In addition, the wind field retrieval algorithm is extended to accommodate the SST factor by adapting the GMFCT for performance validation through wind retrieval. The main contributions of this paper include the following.

1) Based on the characteristics of the HY-2A scatterometer, this paper attempts to construct a GMF containing the SST factor (GMFCT) for the first time by using a

5th-order partial Fourier series containing only cosine terms. This model function adopts the SST as the independent variable and can characterize the quantitative functional relationship between the backscattering coefficient and SST.

2) By analyzing the effect of the SST on the backscattering coefficient, the impact laws of the SST on the backscattering coefficient of the HY-2A scatterometer are revealed, which extends and deepens the understanding of the microwave backscattering behavior of the rough ocean surface.
3) The current scatterometer wind field retrieval algorithm is extended, and a sea surface wind field retrieval algorithm considering the SST is proposed for the HY-2A scatterometer. Experiments show that this algorithm can further improve the wind retrieval accuracy when the SST is considered as input.

The rest of this paper is organized as follows. In section II, we introduce the datasets and methodology, which mainly include the Fourier series and the maximum likelihood estimation (MLE) method. In section III, we use buoy data to verify the accuracy of the European Centre for Medium-Range Weather Forecasts (ECMWF) reanalysis wind field data and introduce the data preprocessing steps. Section IV describes building the GMFCT and then validates it by the wind retrieval data. Section V contains a preliminary discussion of the experimental results. Finally, conclusions are presented in section VI.

II. DATASETS AND METHODOLOGY

This paper uses the L2A data of the HY-2A scatterometer, ECMWF reanalysis wind field data and Tropical Atmosphere Ocean (TAO) buoy data to construct and validate the GMFCT. Data processing can be divided into three stages: 1) Data preprocessing: Before building the GMFCT, the data should be preprocessed, including spatiotemporal matching, outlier rejection, and data sample classification. Finally, the preprocessed data are divided into two parts: the modeling dataset and the validation dataset. 2) Building the GMFCT and GMFWT: the modeling data under different conditions are adopted as input and are fitted by the Fourier series. Then the GMF is obtained. 3) Wind field retrieval: The validation data set is input into the new GMF, and the wind speed and direction of each wind vector cell (WVC) are calculated by the MLE algorithm. The flow chart is shown below. The data, algorithms, and processing steps involved will be described in detail later.

A. DATA SETS

1) SCATTEROMETER DATA

The HY-2A satellite, launched in August 2011, is China's first marine dynamic environmental satellite, which adopts a conically scanning pencil-beam system with two polarized beams, and its operating frequency is the Ku-band. The inner beam is horizontal-horizontal (HH) polarized, and the incident angle is 41°; the outer beam is vertical-vertical (VV) polarized with an incident angle of 48° [27]. In this paper, the L2A data of the HY-2A scatterometer are used for modeling, which have been processed for sigma0s grouping, sea-land and sea-ice identification, atmospheric attenuation correction, etc. [28]. To maximize the storage of the satellite observation data and reduce the storage space, the data are stored along the orbit. The data file of one orbit contains 1,702 rows, and each row contains 76 WVCs. Each WVC contains the backscattering coefficients from different azimuths and polarizations and the corresponding observation time, longitude, latitude, incident angle, azimuth angle, etc. The time range of the L2A data used in this paper is from 2013-01 to 2013-06, and the corresponding orbital number ranges from 06314 to 08808.

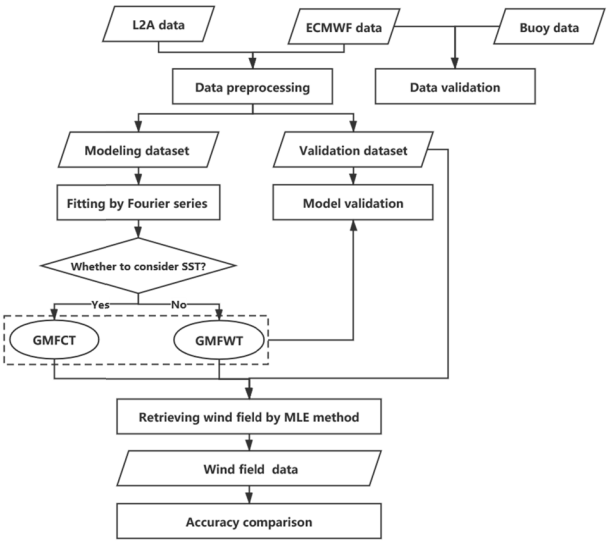

FIGURE 1. Data processing flow chart of this study.

2) ECMWF REANALYSIS WIND FIELD DATA

The ECMWF is an esteemed international research and business organization of weather forecasts established by major European Union countries in 1976. Due to the uneven spatial and temporal distributions of the observation data, the ECMWF uses a relatively complete data assimilation system to reintegrate and optimize the observation data of various types and from various sources, and its products have been widely used in previous atmospheric research [29]. In this paper, the SST, sea surface wind speed, wind direction and rainfall data from the 0.125° × 0.125° high-resolution ECMWF reanalysis data were used, covering a time range from 2013-01 to 2013-06, at time intervals of 3 h.

3) BUOY DATA

At present, buoys are the most important and accurate wind-measuring platform on seas, and can continuously and accurately collect ocean hydrological data. However, the number of buoys is small, and the spatial distribution is

small, so it is difficult for buoys to directly provide enough data for modeling research. In this paper, the TAO buoy data provided by the National Data Buoy Center (NDBC) in the United States, including measured data such as the wind speed and wind direction, were used as the reference standard to verify the accuracy of the ECMWF data before modeling.

B. BUILDING METHOD FOR THE GMFCT

The backscattering coefficient is an even function of the relative wind direction and is symmetric about the 180° relative wind direction. The relative wind direction is defined as the difference between the upwind direction and the radar azimuth. Thus, this study uses a partial Fourier series that contains only cosine terms to characterize the relationship among the backscattering coefficient of the sea surface, SST, sea surface wind vector and radar measurement parameters. A Fourier series can represent any periodic function in terms of an infinite series of sines and cosines and has been widely used in GMF establishment [30], [31]. The specific equation used in the GMFCT modeling is as follows.

$$\begin{aligned}\sigma^0(x) = {} & A_0(w,\theta,p,t) + A_1(w,\theta,p,t)\cdot\cos x \\ & + A_2(w,\theta,p,t)\cdot\cos 2x + A_3(w,\theta,p,t)\cdot\cos 3x \\ & + A_4(w,\theta,p,t)\cdot\cos 4x \end{aligned} \tag{1}$$

where w, x, θ, p and t represent the wind speed, relative wind direction, incident angle, polarization mode and SST, respectively, and A_0, A_1, A_2, A_3 and A_4 are functions of the wind speed, radar incident angle, polarization and SST, respectively. It should be noted that the SST is not considered when building the GMFWT.

After determining that the function to be fitted is a Fourier series, it is important to choose an appropriate fitting method. The least squares method is regarded as a classical numerical optimization method, and it operates by minimizing the square of the error called the residual to determine the most consistent curve with the data. The residual for each observed data-point is usually defined as:

$$\mathrm{e}_i\left(para, \hat{\sigma}_i, x_i\right) = ||\hat{\sigma}_i - \sigma^0(x_i)|| \tag{2}$$

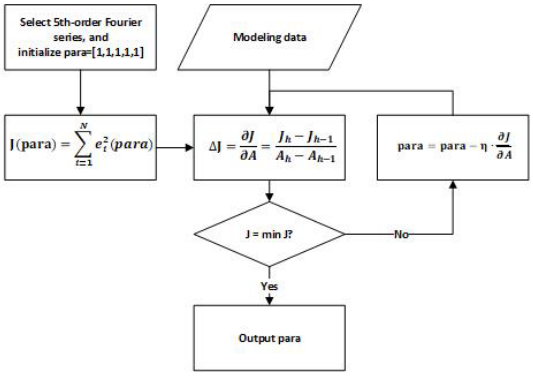

FIGURE 2. Process of building a model by the Fourier series.

where, $\hat{\sigma}_i$ is the measured backscattering coefficient, and para are the coefficients of the Fourier series that need to be solved. In this study, para is [A_0, A_1, A_2, A_3, A_4]. Hence, a minimization algorithm is required to solve the coefficients that minimize the objective function J (para). The objective function can be written as follows:

$$\mathrm{J}(\mathrm{para}) = \sum_{i=1}^{N} e_i^2(para) \tag{3}$$

where N is the total number of data samples involved in modeling under different conditions.

Because a Fourier series is a nonlinear function, it is difficult to derive the objective function directly to obtain the global minimization as the solution. Therefore, the general solution of the nonlinear least squares method is to minimize the objective function through continuous iterative calculations. This study uses the gradient descent method to obtain the optimal solution. The para term is initialized as [1,1,1,1,1]. The whole process of Fourier series fitting is shown in Fig. 2. The gradient calculation equation is as follows:

$$\mathrm{para} = \mathrm{para} - \eta\cdot\frac{\partial J}{\partial A} \tag{4}$$

$$\frac{\partial J}{\partial A}\begin{cases} \dfrac{\partial J}{\partial A_0} = 2\cdot\sum\limits_{i=1}^{N}\left(A_0 + A_1\cdot\cos x_i + A_2\cdot\cos 2x_i + A_3\cdot\cos 3x_i + A_4\cdot\cos 4x_i - \hat{\sigma}_i\right) \\ \dfrac{\partial J}{\partial A_1} = 2\cdot\sum\limits_{i=1}^{N}\left(A_0 + A_1\cdot\cos x_i + A_2\cdot\cos 2x_i + A_3\cdot\cos 3x_i + A_4\cdot\cos 4x_i - \hat{\sigma}_i\right)\cdot\cos x_i \\ \dfrac{\partial J}{\partial A_2} = 2\cdot\sum\limits_{i=1}^{N}\left(A_0 + A_1\cdot\cos x_i + A_2\cdot\cos 2x_i + A_3\cdot\cos 3x_i + A_4\cdot\cos 4x_i - \hat{\sigma}_i\right)\cdot\cos 2x_i \\ \dfrac{\partial J}{\partial A_3} = 2\cdot\sum\limits_{i=1}^{N}\left(A_0 + A_1\cdot\cos x_i + A_2\cdot\cos 2x_i + A_3\cdot\cos 3x_i + A_4\cdot\cos 4x_i - \hat{\sigma}_i\right)\cdot\cos 3x_i \\ \dfrac{\partial J}{\partial A_4} = 2\cdot\sum\limits_{i=1}^{N}\left(A_0 + A_1\cdot\cos x_i + A_2\cdot\cos 2x_i + A_3\cdot\cos 3x_i + A_4\cdot\cos 4x_i - \hat{\sigma}_i\right)\cdot\cos 4x_i \end{cases} \tag{5}$$

where η is the learning rate, and the partial derivative term $\frac{\partial J}{\partial A}$ can be calculated by the following equation (5), as shown at the bottom of the previous page.

C. METHOD FOR RETRIEVING THE SEA SURFACE WIND FIELD

To further verify the accuracy of the GMFCT, it is necessary to conduct wind retrieval experiments using the GMFCT and the validation dataset. In this study, the MLE algorithm was selected for sea surface wind field inversion, which was first proposed by Pierson in 1984 [32]. The MLE method has a deeper theoretical basis for wind field inversion and has the advantages of being completely independent of the GMF. In addition, it has no limitations regarding the units and range of the backscattered measurement values. Regardless of the unit of the backscattered measurement, the algorithm performs well. This algorithm has been successfully applied to the inversion of the sea surface wind field from ERS/SCAT and NSCAT scatterometers, and it is the most widely used inversion method among the operational satellites [33]–[35]. To conform to the GMFCT, the MLE algorithm also needs to include the SST factor. The extended objective function is as follows:

$$J_{MLE}(w, \Phi) = -\sum_{i=1}^{N}\left[\frac{(z_i - M(\mathrm{w}, \Phi - \phi_i, \theta_i, p_i, t_i))^2}{2V_{R_i}} + ln\sqrt{V_{R_i}}\right] \quad (6)$$

where N is number of measured values of the backscattering coefficient in each WVC, R_i is the deviation of the ith measured value from the model value, V_{R_i} is the total deviation variance, z is the measured value of the radar backscattering coefficient, M is the radar backscattering coefficient predicted by the model function under certain conditions, and w, Φ, ϕ, θ, p and t are the wind speed, upwind direction, radar observation azimuth, incident angle, polarization mode and SST, respectively. The variance in the total error V_R is determined by the model function and the characteristics of the scatterometer system and is a function of the design parameters and measurement parameters of the scatterometer. Wind field inversion is actually applied to determine the wind vectors that result in a local maximum of equation (6). In practice, there are generally 2-4 local maxima of the objective function when inverting the wind field, and each local maximum value represents a possible wind vector solution, also known as the wind vector ambiguity. In this paper, to remove false ambiguities to obtain the final real result, we adopt the ECMWF wind direction as the true reference and choose the ambiguity with the wind direction closest to that of the ECMWF as the true wind vector solution.

D. STATISTICAL METHODS

To verify the accuracy of the GMF and wind field inversion algorithm, the mean absolute deviation (MAD), mean deviation (MD) and root mean square (RMS) are calculated. We define x_i as the predicted or retrieved value, y_i as the observed or reference value, and N as the total number of data samples.

Then, the MAD is defined as:

$$|\bar{E}| = \frac{1}{N}\sum_{i=1}^{N}|x_i - y_i| \quad (7)$$

The MD is defined as:

$$\bar{E} = \frac{1}{N}\sum_{i=1}^{N}(x_i - y_i) \quad (8)$$

The RMS is defined as:

$$E_{rms} = \sqrt{\frac{1}{N}\sum_{i=1}^{N}(x_i - y_i)^2} \quad (9)$$

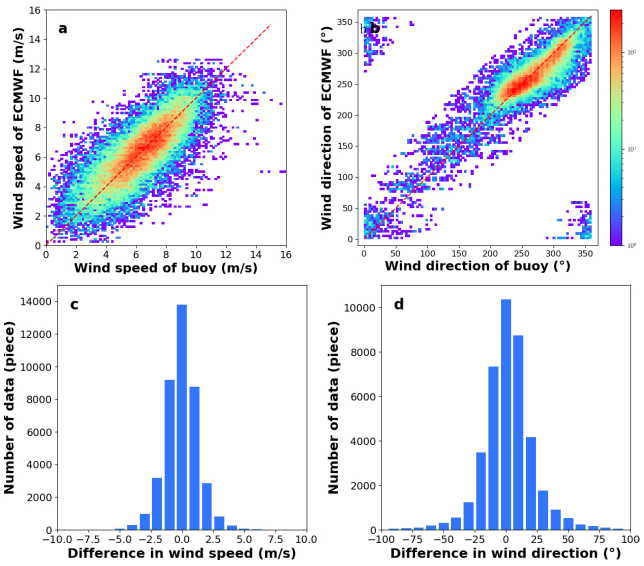

FIGURE 3. Evaluation of the ECMWF wind speed and direction accuracy with the TAO buoy data as the reference. (a) Scatter plot of the wind speeds from the ECMWF and TAO; (b) scatter plot of the wind directions from the ECMWF and TAO; (c) distribution of the wind speed deviation; (d) distribution of the wind direction deviation.

III. DATA ACCURACY VERIFICATION AND PREPROCESSING

A. VERIFICATION OF THE ACCURACY OF THE ECMWF REANALYSIS WIND FIELD DATA

The time range of the ECMWF data used to test the accuracy of the wind speed and direction is from 2013-01 to 2013-06. It is matched against TAO buoy data with a spatial window of 0.125° and a time window of 0.5 h. First, the buoy data that are anomalous or affected by rain are removed, and the 4-m reference height wind speed of the buoy is then converted into the 10-m neutral wind speed by the LKB function [36]. Finally, approximately 40,297 data samples of the wind speed in the range of [3 m/s, 15 m/s] are selected to test the accuracy of the ECMWF data. The results are shown in Fig.3. After statistical analysis, the MD and RMS between the wind speed

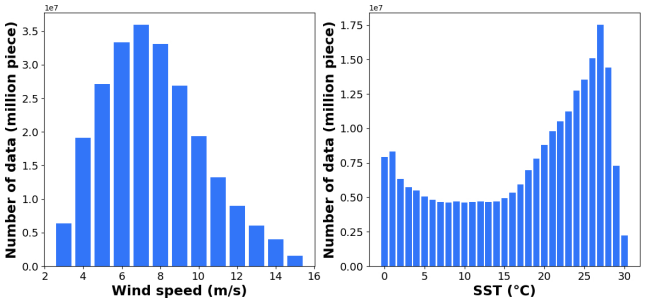

FIGURE 4. Histogram of the sample data.

of the ECMWF reanalysis wind field data and that of the TAO buoy data are 0.037 and 1.315 m/s, respectively, and the MD and RMS of the wind direction data are 1.937° and 19.802°, respectively. The RMS error of the wind speed is within 2 m/s, and the RMS error of the wind direction is within 20°, which approximately follows a normal distribution with a mean of zero. The results show that the ECMWF reanalysis wind field data satisfy the accuracy requirements and can be used to construct the GMF.

B. PREPROCESSING OF THE EXPERIMENTAL DATA

When matching the ECMWF data with the L2A data from the HY-2A scatterometer, adopting the L2A WVCs as the reference cells, the nearest point spatially and temporally to the ECMWF data is selected as the matching point with a spatial window of 0.125° and a temporal window of 0.5 h. Then, the data polluted by rainfall should be removed. Because the HY-2A scatterometer uses the Ku microwave band to measure the wind and the Ku-band is greatly disturbed by rainfall, including the influence of raindrop attenuation, raindrop backscattering and raindrop surface disturbance [37], data with rainfall levels higher than 0.1 mm/h are removed from the experiment.

Qiu from the South China Sea Prediction Center of the State Oceanic Administration once verified the accuracy of the wind field retrieved by the HY-2A scatterometer and found that when the wind speed was lower than 3 m/s, the backscattering coefficient measured by the HY-2A scatterometer contained more noise [38]. Furthermore, when the wind speed was higher than 15 m/s, there were few well-matched sample data. Therefore, the wind speed range of this experiment is limited to 3-15 m/s. The SST range is limited to 0-30°C because the SSTs in most of the data samples are within this range. Finally, approximately 230 million data match-ups are selected under these conditions. For each polarization, the data are classified by the wind speed, SST and relative wind direction with intervals of 0.1 m/s, 1°C, and 1°, respectively, thus constituting the dataset of this experiment. The data with a time range of 2013-01-01 to 2013-06-15 are used for modeling, and those from 2013-06-15 to 2013-06-30 are used to verify the accuracy of the model. The distribution of the classified data with the temperature and wind speed is shown in Fig.4.

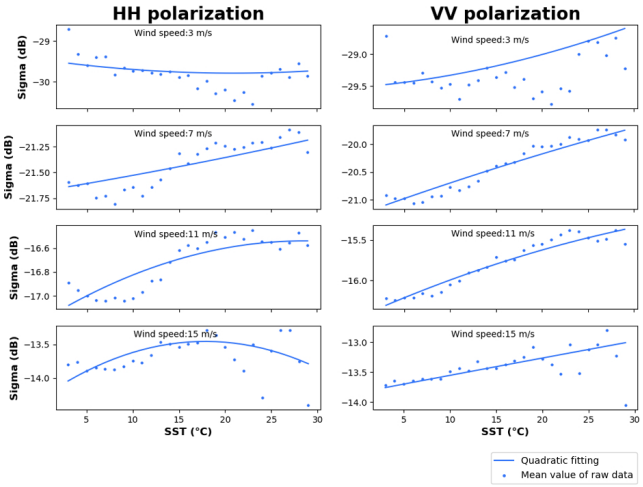

FIGURE 5. Under HH and VV polarization, the backscattering coefficients at the different wind speeds vary with the SST.

IV. RESULTS AND ANALYSIS

A. INFLUENCE OF THE SST ON THE GMF

Although the total number of data points used in this experiment is large, the distribution is relatively concentrated. As shown in Fig. 4, the amount of data at the low-, medium- and high-wind speeds accounts for 16.25%, 66.42% and 17.33%, respectively, of all data and the temperatures are mainly concentrated between approximately 1°C and 27°C, so classifying the dataset by the wind speed, SST, and relative direction at intervals 0.1 m/s, 1°C, and 1°, respectively, will lead to too little data in some classifications. Additionally, because of the measurement noise from the HY-2A scatterometer, there are some data samples with large deviations in each class. To avoid the influence of outliers, the experiment uses the mean value in each class to perform statistical analysis, and the results are shown in Fig. 5. Some wind speed intervals have large fluctuations at low and high temperatures, especially at high wind speeds. If using a Fourier series to fit the models of the different temperatures in each wind speed interval, some models cannot be fitted very well under certain conditions due to insufficient data and quality problems. Therefore, the idea of this paper is to use the sufficient data at three different temperatures (5°C, 15°C and 25°C) at each wind speed for model fitting, while the backscattering coefficients at the other temperatures are obtained by interpolating between these three curves. At the same wind speed and relative wind direction, the backscattering coefficient does not always change monotonically with the temperature, and an inflection point will occur when reaching a certain temperature under certain conditions. Therefore, quadratic interpolation is applied to estimate the backscattering coefficient at the other temperatures. The GMFCT fitting results are summarized in Tables 1 and 2, and two examples of the fitting results are shown in Fig. 6, one for HH polarization, and the other for VV polarization both at the wind speed of 7 m/s and the SST of 15 °C. In Fig. 6, the blue dots represent

TABLE 1. Fitting results at the different wind speeds and temperatures under HH polarization.

Wind speed (m/s)	SST (°C)	A0	A1	A2	A3	A4
	5	-28.1132	2.0135	0.9000	0.1399	-0.0253
4	15	28.0864	2.0693	1.0251	-0.1394	-0.3120
	25	-27.9561	2.0921	1.4535	-0.0141	-0.0296
	5	-21.7930	1.6774	1.4849	-0.0844	-0.2422
7	15	-21.4910	1.5667	1.6513	-0.0514	-0.1811
	25	-21.4131	1.5374	1.8279	-0.0764	-0.2171
	5	-18.0103	1.3784	1.9147	-0.1257	-0.1755
10	15	-17.6997	1.2866	1.9775	-0.0733	-0.3176
	25	-17.5653	1.3153	1.9288	-0.0347	-0.2214
	5	-15.4499	1.0714	1.9462	-0.2037	-0.0737
13	15	-15.0248	1.1491	1.8185	-0.1525	-0.1533
	25	-15.1160	1.1090	1.8762	-0.0948	-0.1350

TABLE 2. Fitting results at the different wind speeds and temperatures under VV polarization.

Wind speed (m/s)	SST (°C)	A0	A1	A2	A3	A4
	5	-27.8727	0.9889	1.6061	-0.1859	-0.0954
4	15	-27.5314	0.9159	1.7107	-0.0629	-0.4132
	25	-27.0938	0.9022	2.2083	-0.1079	-0.2586
	5	-21.2297	0.5872	2.6373	-0.1095	-0.4513
7	15	-20.6375	0.4835	2.6991	-0.0713	-0.5471
	25	-20.1091	0.5520	2.9257	-0.0434	-0.5625
	5	-17.1179	0.5562	2.7184	-0.1230	-0.5325
10	15	-16.6961	0.4612	2.6441	-0.0620	-0.5767
	25	-16.3159	0.5648	2.5859	-0.0479	-0.5951
	5	-14.9046	0.5124	2.1950	-0.1097	-0.4217
13	15	-14.5737	0.5529	2.1014	-0.1637	-0.3616
	25	-14.3263	0.43499	2.0786	-0.0146	-0.3923

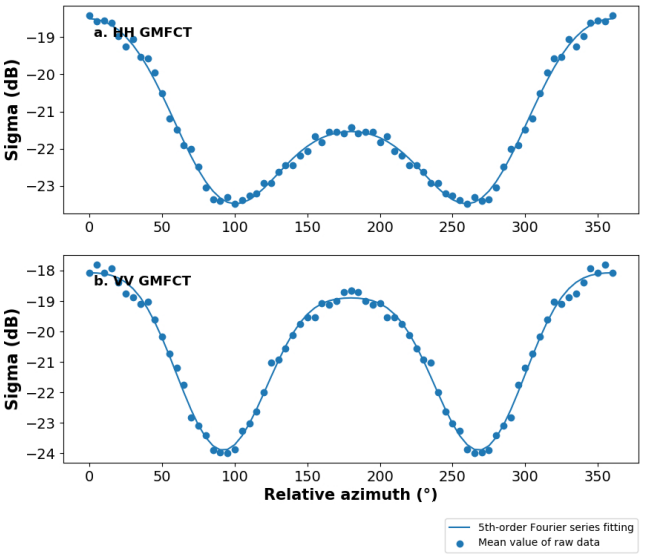

FIGURE 6. Fitting results of the GMF for the wind speed of 7m/s and the SST of 15 °C.

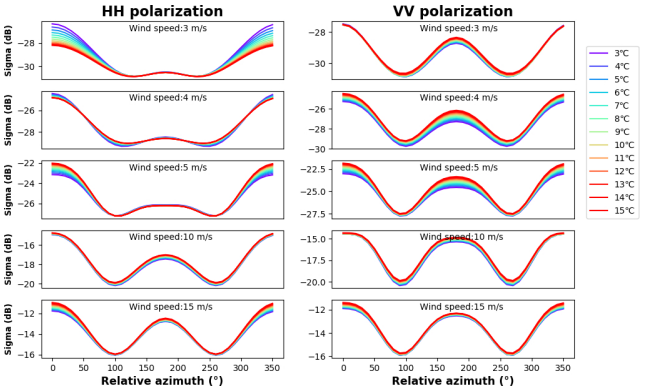

FIGURE 7. Curves of the GMF including the SST under the different wind speed conditions and HH and VV polarization.

the mean value of the data samples in each relative azimuth interval, while the solid blue lines are the model curves fitted by the 5th-order Fourier series method. As shown in this figure, the Fourier series method has achieved good fitting effect. In addition, to assess the effect of the SST on the accuracy of the model, a geophysical model without the SST factor (GMFWT) is also constructed with the same dataset.

As shown in Fig. 7, the curves of the GMFCT under the two polarizations are w-shaped, which is similar to the previously developed GMF. The curves at the same wind speed are clustered, and each cluster of curves consists of 13 different temperature curves at temperature intervals of 1°C. The figure reveals that the curves at the same wind speed show a notably regular distribution, and these curves are not concentrated at a certain position, which illustrates that the SST has a certain impact on the backscattering coefficient. The regularity is manifested as follows: in the low-wind speed section, the backscattering coefficient has no clear correlation with the SST, but with increasing wind speed, the backscattering coefficient gradually becomes positively correlated with the temperature, and the wind speed at which the change occurs is approximately 4 m/s. In addition, with increasing wind speed, the curve gradually becomes concentrated, and the distribution width decreases, indicating that the influence of the SST on the backscattering coefficient also depends on the wind speed. The higher the wind speed is, the lower the impact of the SST is on the backscattering coefficient. There is no significant correlation between the backscattering coefficient and the SST in the low-wind speed section, which may be related to the sensor noise because the signal-to-noise ratio of the HY-2A scatterometer is lower at low wind speeds, which impacts the data quality.

To analyze the accuracy of the GMFCT and the improvement of the SST in wind field inversion, data from 2013-06-15 to 2013-06-30 were input into the GMFCT model to calculate the backscattering coefficients at the different temperatures and different wind speeds and were compared to the results of the GMFWT and the HY-2A-measured data. For brevity, the following table only shows the backscattering coefficients for 0°C and 30°C at each wind speed of the GMFCT. The calculated results show that, except for the wind speeds of 3 and 4 m/s under HH polarization and wind

TABLE 3. Comparison of the GMFCT, GMFWT and measured data under HH polarization.

Wind speed (m/s)	GMFCT		GMFWT	HY-2A
	0°C	30°C		
3	-28.618	-29.114	-29.056	-29.674
4	-27.607	-27.536	-27.216	-27.592
5	-25.679	-25.221	-24.989	-25.255
6	-23.518	-23.082	-22.991	-23.188
7	-21.600	-21.245	-21.287	-21.445
8	-20.208	-19.602	-19.861	-19.986
9	-19.121	-18.529	-18.642	-18.729
10	-17.992	-17.480	-17.576	-17.656
11	-17.051	-16.545	-16.644	-16.719
12	-16.372	-15.912	-15.694	-15.777
13	-15.587	-14.462	-14.963	-15.029
14	-14.715	-13.729	-14.236	-14.313
15	-14.040	-12.840	-13.544	-13.675

TABLE 4. Comparison of the GMFCT, GMFWT and measured data under VV polarization.

Wind speed (m/s)	GMFCT		GMFWT	HY-2A
	0°C	30°C		
3	-29.223	-28.263	-28.993	-29.228
4	-27.975	-26.756	-27.038	-27.045
5	-25.599	-24.149	-24.604	-24.607
6	-23.508	-21.824	-22.351	-22.358
7	-21.233	-19.825	-20.435	-20.437
8	-19.515	-18.124	-18.872	-18.874
9	-18.271	-16.967	-17.610	-17.608
10	-17.104	-16.066	-16.622	-16.622
11	-16.427	-15.404	-15.804	-15.805
12	-15.594	-14.699	-15.116	-15.120
13	-14.976	-13.980	-14.457	-14.459
14	-14.205	-12.787	-13.898	-13.891
15	-13.766	-13.051	-13.428	-13.436

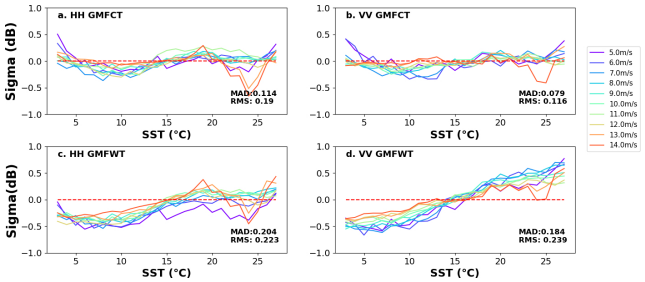

FIGURE 8. Variation curve of the backscattering coefficient error with the SST under the different wind speed conditions. a and b are the GMFCT under HH and VV polarization, respectively; c and d are the GMFWT under HH and VV polarization, respectively.

speeds of 3 m/s under VV polarization, the mean backscattering coefficients of the GMFWT and the HY-2A-measured data nearly fall between the backscattering coefficients at the highest and lowest temperatures of the GMFCT, indicating that the GMFCT can better reflect the influence of the SST on the backscattering coefficient.

Fig. 8 shows the changes in the bias errors between the backscattering coefficients of the GMFCT/GMFWT and the

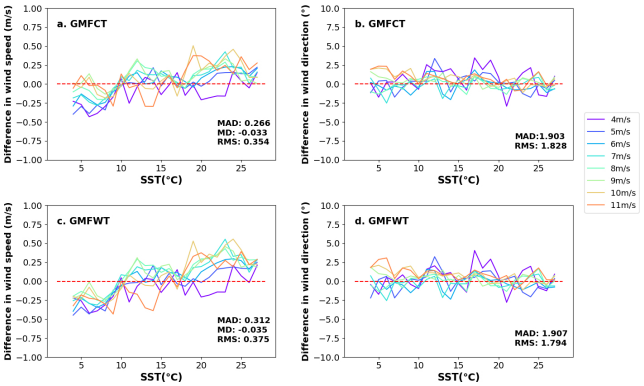

FIGURE 9. Comparison of the GMFCT and GMFWT inversion accuracies of the sea surface wind field under HH polarization. a and b are the error changes for the wind speed and direction inversion, respectively, by the GMFCT; c and d are the error changes for the wind speed and direction inversion, respectively, by the GMFWT.

backscattering coefficients measured by the HY-2A scatterometer (the measured value minus the model value) with the SST under the different wind speed conditions, which clearly reflects the influence of the SST on the GMF under the different wind speed conditions. As shown in Fig. 8, after considering the SST factor, the accuracy of the backscattering coefficient calculated by the GMF has been clearly improved. The MAD of the backscattering coefficient under HH polarization is reduced 44.1%, and the MAD of the backscattering coefficient under VV polarization is reduced 57.8%, indicating that the backscattering coefficient measured under VV polarization is more strongly affected by the SST than that under HH polarization. Under the two polarizations, the bias error curve of the backscattering coefficient at most wind speeds crosses the 0 line at approximately 18°C. Under VV polarization, the farther away from the cross-point temperature, the larger the absolute error is, whereas the bias error under HH polarization does not change notably with the distance from the cross-point, indicating that the backscattering coefficient measured under VV polarization is more sensitive to the SST.

B. INFLUENCE OF THE SST ON SEA SURFACE WIND FIELD INVERSION

The GMFCT and GMFWT are used to invert the wind field, and the retrieved results are compared to the validation data. The validation data are the wind vector data from the ECMWF reanalysis product. The time range of the HY-2A satellite scatterometer data used to retrieve the wind field spans from 2013-06-15 to 2013-06-30. After removing the data affected by rainfall and anomalous data points (the difference between the retrieved wind direction and the ECMWF wind direction is larger than 90°) [39], approximately 2.3 million data samples of the wind speed in the range of [3 m/s, 15 m/s] are obtained. Because the wind direction deviation is not significant, the MD is not calculated for the wind direction. The statistical results are shown in Figs. 9 and 10. It is evident that the GMFCT realizes a clear

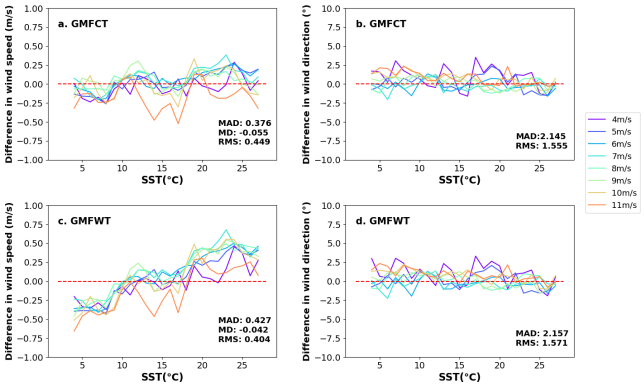

FIGURE 10. Comparison of the GMFCT and GMFWT inversion accuracies of the sea surface wind field under VV polarization. a and b are the error changes for the wind speed and direction inversion, respectively, by the GMFCT; c and d are the error changes for the wind speed and direction inversion, respectively, by the GMFWT.

TABLE 5. Variations in the mean error of the GMFCT and GMFWT with the temperature.

Pol	Model	SST					
		6°C	10°C	14°C	18°C	22°C	26°C
HH	GMFCT	-0.256	-0.093	-0.078	-0.05	0.202	0.051
	GMFWT	-0.349	-0.140	-0.081	-0.014	0.281	0.166
VV	GMFCT	-0.245	-0.100	-0.210	-0.060	0.145	-0.019
	GMFWT	-0.467	-0.200	-0.192	0.067	0.379	0.3267

correction effect on the accuracy of wind speed inversion. Under HH polarization, the MAD of the wind speed reduced 14.7%, and the MD exhibits no notable change. The MAD of the wind direction decreases by 0.99%. From the statistical data under VV polarization, the MAD of the wind speed is reduced 11.9%, and the MD is slightly increased. However, from the curve of the wind speed error versus the temperature, it is clear that the error curve of the GMFCT is more horizontal and fluctuates around the zero value line, whereas the error curve of the GMFWT has an upward trend with increasing temperature, indicating that the SST has a certain corrective effect on the systematic deviation in wind speed inversion. In summary, the SST has a certain correction effect on the accuracy of the retrieved sea surface wind field, but the improvement in the wind direction is not notable. Moreover, the abovementioned phenomenon whereby VV polarization is more sensitive to the SST is also demonstrated in wind field inversion.

V. DISCUSSION

From the above experiments, the influence of the SST on the backscattering coefficient is described as follows: at low wind speeds, there is a negative correlation between the backscattering coefficient and SST, but as the wind speed increases, it gradually becomes a positive correlation. At the same time, the backscattering coefficient curve gradually becomes concentrated, and the distribution width decreases with increasing wind speed. The following is a preliminary discussion on the main causes and physical mechanisms of these phenomena.

The microwave radiation characteristics of ocean water depend on two main factors: the dielectric constant and sea surface roughness. On the one hand, the scattering process of seawater mainly involves surface scattering, and the scattering intensity and the dielectric constant of the ocean surface are positively correlated. The dielectric constant of seawater is a function of the temperature and salinity. When the salinity is constant, the dielectric constant of seawater and the temperature are negatively correlated, but the effect is very limited [40]. Therefore, in theory, the higher the SST is, the smaller the seawater dielectric constant, and backscattering coefficient are; On the other hand, the roughness of the sea surface reflects the degree of scattering in the radiated area. The sea surface at a low wind speed is dominated by specular reflection, whereas at a high wind speed, the sea surface is rough with capillary waves, which enhance the intensity of the radar backscatter. Generally, the higher the wind speed over the sea surface is, the rougher the sea surface is and the larger the backscattering coefficient is, which is also the basis for wind measurement by scatterometers. Many factors influence the sea surface roughness, such as the wind speed, seawater density, and viscosity [41], [42]. Among them, the seawater viscosity strongly correlated with the temperature. The empirical relationship between these two parameters can be fitted using a quadratic polynomial, which reveals a negative correlation, and the correlation coefficient can reach approximately 0.9 [43]. Therefore, when the wind speed remains constant, the higher the temperature is, the smaller the seawater viscosity is, the rougher the sea surface is, and the larger the backscattering coefficient is.

There are at least two mechanisms for the influence of the temperature on the backscattering coefficient: (1) temperature affects the dielectric constant, and the backscattering coefficient decreases with increasing temperature; (2) temperature affects the seawater viscosity, and the backscattering coefficient increases with the decreasing seawater viscosity as well as increasing temperature. At present, it seems that these two influence mechanisms of the temperature on the backscattering coefficient are contradictory, so the final effect depends on which mechanism is dominant. From the experimental results, according to the second mechanism, the influence of the seawater viscosity on the sea surface roughness requires wind participation. Therefore, at low wind speeds, the influence of the wind is limited, and the influence of the dielectric constant dominates, causing a negative correlation between the backscattering coefficient and temperature; However, as the wind speed increases, the sea surface gradually changes from a smooth surface to a rough surface, and the temperature has a small effect on the dielectric constant of the seawater, so the roughness gradually becomes dominant, and the backscattering coefficient increases with increasing temperature. In addition, the higher the wind speed is, the greater its contribution to the sea surface roughness is, which weakens the temperature effect. Therefore, as the wind

speed increases, the backscattering coefficient curves at the different temperatures gradually become concentrated, and the distribution width decreases.

VI. CONCLUSION

In this paper, the L2A data of the HY-2A scatterometer and the corresponding ECMWF data are used to build a GMF containing the SST by the Fourier series method. The following three conclusions are obtained through the experiments:

First, the responses of the backscattering coefficient under the two polarizations to the SST are different. After the SST is considered in the GMFCT, the MAD of the backscattering coefficient under HH polarization is reduced 44.1%, and the MAD under VV polarization is reduced 57.8%. The systematic deviation of the backscattering coefficient measured under VV polarization is corrected more than that under HH polarization, which indicates that VV polarization is more sensitive to the SST than HH polarization.

Second, the accuracy of the wind field retrieved by the GMF containing the SST is considerably improved, and the systematic deviation in the wind speed is effectively corrected; thus, the GMFCT has a great potential for improving the wind quality retrieved by the scatterometer.

Finally, the Fourier series method is a feasible method to build the GMF containing the SST for the HY-2A scatterometer. Although there are not much data and the data are noisy under certain conditions, a smooth model curve can still be obtained through a fifth-order Fourier series.

However, it should be pointed out that the discussion on the mechanism of the SST effect on the scatterometer wind measurements is only a preliminary examination and has not yet been verified. Hence, further research is needed.

ACKNOWLEDGMENT

The authors would like to thank the European Centre for Medium-Range Weather Forecasts (ECMWF) and the National Data Buoy Center (NDBC) for providing the reanalysis wind field data and buoy data, respectively.

REFERENCES

[1] Z. Wang, C. Zhao, J. Zou, X. Xie, Y. Zhang, and M. Lin, "An improved wind retrieval algorithm for the HY-2A scatterometer," *Chin. J. Oceanol. Limnol.*, vol. 33, no. 5, pp. 1201–1209, Sep. 2015.

[2] X. Ye, M. Lin, X. Yuan, J. Ding, X. Xie, Y. Zhang, and Y. Xu, "Satellite SAR observation of the sea surface wind field caused by rain cells," *Acta Oceanologica Sinica*, vol. 35, no. 9, pp. 80–85, Sep. 2016.

[3] A. C. P. Oude Nijhuis, O. K. Krasnov, C. M. H. Unal, H. W. J. Russchenberg, and A. Yarovoy, "Outlook for a new wind field retrieval technique: The 4D-Var wind retrieval," in *Proc. Int. Radar Conf.*, Lille, France, Oct. 2014, pp. 1–6.

[4] D. G. Long, "Polar applications of spaceborne scatterometers," *IEEE J. Sel. Topics Appl. Earth Observ. Remote Sens.*, vol. 10, no. 5, pp. 2307–2320, May 2017.

[5] L. Zhang, Q. Zhang, B. Du, X. Huang, Y. Y. Tang, and D. Tao, "Simultaneous spectral-spatial feature selection and extraction for hyperspectral images," *IEEE Trans. Cybern.*, vol. 48, no. 1, pp. 16–28, Jan. 2018.

[6] F. Luo, L. Zhang, B. Du, and L. Zhang, "Dimensionality reduction with enhanced hybrid-graph discriminant learning for hyperspectral image classification," *IEEE Trans. Geosci. Remote Sens.*, early access, Jan. 27, 2020, doi: 10.1109/TGRS.2020.2963848.

[7] F. Luo, H. Huang, Y. Duan, J. Liu, and Y. Liao, "Local geometric structure feature for dimensionality reduction of hyperspectral imagery," *Remote Sens.*, vol. 9, no. 8, p. 790, Aug. 2017.

[8] S. H. Yueh, B. W. Stiles, and W. T. Liu, "QuikSCAT geophysical model function and winds for tropical cyclones," in *Proc. Microw. Remote Sens. Atmos. Environ. III*, Hangzhou, China, Apr. 2003, pp. 206–217.

[9] J. Zou, T. Zeng, and S. Cui, "A high wind geophysical model fuction for QuikSCAT wind retrievals and application to typhoon IOKE," *Acta Oceanologica Sinica*, vol. 34, no. 7, pp. 65–73, Jul. 2015.

[10] R. Singh, P. Kumar, and P. K. Pal, "Assimilation of oceansat-2-scatterometer-derived surface winds in the weather research and forecasting model," *IEEE Trans. Geosci. Remote Sens.*, vol. 50, no. 4, pp. 1015–1021, Apr. 2012.

[11] M. Zheng, X.-M. Li, and J. Sha, "Comparison of sea surface wind field measured by HY-2A scatterometer and WindSat in global oceans," *J. Oceanol. Limnol.*, vol. 37, no. 1, pp. 38–46, Jan. 2019.

[12] A. Stoffelen and D. Anderson, "Scatterometer data interpretation: Measurement space and inversion," *J. Atmos. Ocean. Technol.*, vol. 14, no. 6, pp. 1298–1313, Dec. 1997.

[13] Y. Quilfen, B. Chapron, T. Elfouhaily, K. Katsaros, and J. Tournadre, "Observation of tropical cyclones by high-resolution scatterometry," *J. Geophys. Res., Oceans*, vol. 103, no. C4, pp. 7767–7786, Apr. 1998.

[14] H. Hersbach, A. Stoffelen, and S. D. Haan, "An improved C-band scatterometer ocean geophysical model function: CMOD5," *J. Geophys. Res. Oceans.*, vol. 112, no. C3, pp. 5767–5780, Oct. 2006.

[15] A. Stoffelen, J. A. Verspeek, J. Vogelzang, and A. Verhoef, "The CMOD7 geophysical model function for ASCAT and ERS wind retrievals," *IEEE J. Sel. Topics Appl. Earth Observ. Remote Sens.*, vol. 10, no. 5, pp. 2123–2134, May 2017.

[16] L. Ricciardulli and F. J. Wentz, "A scatterometer geophysical model function for climate-quality winds: QuikSCAT ku-2011," *J. Atmos. Ocean. Technol.*, vol. 32, no. 10, pp. 1829–1846, Oct. 2015.

[17] F. M. Monaldo, D. R. Thompson, W. G. Pichel, and P. Clemente-Colon, "A systematic comparison of QuikSCAT and SAR ocean surface wind speeds," *IEEE Trans. Geosci. Remote Sens.*, vol. 42, no. 2, pp. 283–291, Feb. 2004.

[18] J. Zhong, S. Huang, and L. Zhang, "Research on the development of surface wind retrieval from microwave scatterometer," *Scientia Meteorologica Sinica.*, vol. 30, no. 1, pp. 137–142 Feb. 2010.

[19] W. T. Liu, "The effects of the variations in sea surface temperature and atmospheric stability in the estimation of average wind speed by SEASAT-SASS," *J. Phys. Oceanogr.*, vol. 14, no. 2, pp. 392–401, Feb. 1984.

[20] G. T. Lleonart and D. R. Blackman, "The spectral characteristics of wind-generated capillary waves," *J. Fluid Mech.*, vol. 97, no. 3, pp. 455–479, Apr. 1980.

[21] S. A. Grodsky, V. N. Kudryavtsev, A. Bentamy, J. A. Carton, and B. Chapron, "Does direct impact of SST on short wind waves matter for scatterometry?" *Geophys. Res. Lett.*, vol. 39, no. 12, pp. L12602–L12608, Jun. 2012.

[22] N. Ebuchi, "Sea surface temperature dependence of C-band radar cross sections observed by ERS-1/AMI scatterometer," *J. Adv. Mar. Sci. Technol. Soc.*, vol. 3, no. 2, pp. 157–168, Dec. 1997.

[23] X. Xie, K. Chen, and L. Guo, "Research on modeling of ocean water geophysical model function including ocean surface temperature," *J. Tropical Oceanogr.*, vol. 26, no. 6, pp. 14–20, Nov. 2007.

[24] Z. Wang, A. Stoffelen, C. Zhao, J. Vogelzang, A. Verhoef, J. Verspeek, M. Lin, and G. Chen, "An SST-dependent ku-band geophysical model function for RapidScat," *J. Geophys. Res., Oceans*, vol. 122, no. 4, pp. 3461–3480, Apr. 2017.

[25] D. Pan and Y. Bai, "Satellite remote sensing of marine environment and future plan in China," in *Proc. Remote Sens. Inland, Coastal, Ocean. Waters*, Yunnan, China, Dec. 2008, pp. 3–10.

[26] Q. Zhang and L. Zhao, "A review of the development of Chinese marine satellites," *Satell. Appl.*, vol. 77, no. 5, pp. 30–33, May 2018.

[27] B. Mu, M. Lin, and H. Peng, "Validation of wind vectors retrieved by the HY-2 microwave scatterometer using NCEP model data," *Eng. Sci.*, vol. 16, no. 6, pp. 39–45, Apr. 2014.

[28] Y. Lin, J. Zou, and Y. He, "Design of data processing software for HY-2 satellite microwave scatterometer," *Mar. Sci. Bull.*, vol. 35, no. 4, pp. 443–448, Aug. 2016.

[29] K. E. Trenberth and J. G. Olson, "An evaluation and intercomparison of global analyses from the national meteorological center and the European centre for medium range weather forecasts," *Bull. Amer. Meteorolog. Soc.*, vol. 69, no. 9, pp. 1047–1057, Sep. 1988.

[30] X. Xie, Y. Fang, Y, and K. Chen, "A fast wind vector search algorithm for ocean surface wind retrival," *J. Remote Sens.*, vol. 10, no. 2, pp. 236–241, Mar. 2006.
[31] F. J. Wentz, S. Peteherych, and L. A. Thomas, "A model function for ocean radar cross sections at 14.6 GHz," *J. Geophys. Res.*, vol. 89, no. C3, pp. 3689–3704, May 1984.
[32] W. J. Pierson, "A Monte Carlo comparison of the recovery of winds near upwind and downwind from the SASS-1 model function by means of the sum of squares algorithm and a maximum likelihood estimator," NASA, Washington, DC, USA, Tech. Rep. NASA-CR-3839, Oct. 1984.
[33] A. G. Fore, B. W. Stiles, A. H. Chau, B. A. Williams, R. S. Dunbar, and E. Rodriguez, "Point-wise wind retrieval and ambiguity removal improvements for the QuikSCAT climatological data set," *IEEE Trans. Geosci. Remote Sens.*, vol. 52, no. 1, pp. 51–59, Jan. 2014.
[34] X. Xie, Y. Fang, and X. Chen, "Research on numercial wind retrieval algorithm based on maxinum likelihood estimation," *Geography Geo-Inf. Sci.*, vol. 21, no. 1, pp. 30–33, Jan. 2005.
[35] X. Xie, Z. Huang, M. Lin, K. Chen, Y. Lan, X. Yuan, X. Ye, and J. Zou, "A novel integrated algorithm for wind vector retrieval from conically scanning scatterometers," *Remote Sens.*, vol. 5, no. 12, pp. 6180–6197, Nov. 2013.
[36] W. T. Liu and W. Tang, "Equivalent neutral wind," Jet Propuls. Lab., Pasadena, CA, USA, Tech. Rep. 96-17, Aug. 1996.
[37] B. W. Stiles and S. H. Yueh, "Impact of rain on spaceborne Ku-band wind scatterometer data," *IEEE Trans. Geosci. Remote Sens.*, vol. 40, no. 9, pp. 1973–1983, Sep. 2002.
[38] Y. Qiu, D. Xu, and X. Lu, "Validation and analysis of wind field from HY-2A scatterometer in the South China Sea," *Mar. Forecasts.*, vol. 35, no. 4, pp. 25–33, Aug. 2018.
[39] N. Ebuchi, H. C. Graber, and M. J. Caruso, "Evaluation of wind vectors observed by QuikSCAT/SeaWinds using ocean buoy data," *J. Atmos. Ocean. Technol.*, vol. 19, no. 12, pp. 2049–2062, Dec. 2002.
[40] E. H. Grant and R. Shack, "Complex permittivity measurements at 8 6 mm wavelength over the temperature range 1-60 c," *Brit. J. Appl. Phys.*, vol. 18, no. 12, pp. 1807–1814, Dec. 1967.
[41] W. T. Liu, K. B. Katsaros, and J. A. Businger, "Bulk parameterization of air-sea exchanges of heat and water vapor including the molecular constraints at the interface," *J. Atmos. Sci.*, vol. 36, no. 9, pp. 1722–1735, Sep. 1979.
[42] P. K. Taylor and M. J. Yelland, "The dependence of sea surface roughness on the height and steepness of the waves," *J. Phys. Oceanogr.*, vol. 31, no. 2, pp. 572–590, Feb. 2001.
[43] X. Li, R. Lin, and W. Xu, "Experimental study on the thermophysical properties of sea water in the Yellow Sea," *Chem. Eng. Equip.*, vol. 3, no. 5, pp. 4–7, May 2017.

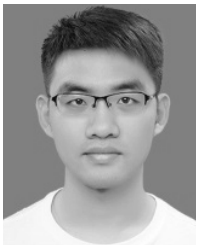

YIHUAN PENG was born in Guangdong, China, in 1993. He received the B.S. degree from Guangzhou University, in 2017, where he is currently pursuing the M.S. degree. He has been participating in the development of data processing system of the Chinese HY-2 series satellites, since 2017. His research interests include microwave remote sensing, data analysis, and algorithms design and engineering.

XUETONG XIE received the Ph.D. degree in cartography and geographical information system from the Institute of Remote Sensing and Geographical Information System, Peking University, Beijing, China, in 2007. He had ever been a designer in charge of the Chinese HY-2A satellite scatterometer data processing with National Satellite Ocean Application Service, Beijing. He played an important role in model and algorithm developing and the data processing software designing for the HY-2A satellite scatterometer. He is currently an Associate Professor with Guangzhou University. His research interests include microwave scatterometer data processing, simulation, and ocean wind retrieval.

MINGSEN LIN (Member, IEEE) received the Ph.D. degree in computing mathematics from the Computing Center, Chinese Academy of Sciences, Beijing, China, in 1992. He is currently the Chief Designer of ground application system for HY-1 and HY-2 satellites, where he organized the argument of Chinese Ocean Satellite outline, and managed the construction of ground application system for the Chinese Ocean Satellite with National Satellite Ocean Application Service, Beijing. He is also the Founder of satellite ocean remote sensing in China. He plays an important role in the development of Chinese Ocean Satellite and Manned Space Flight. His research interests include remote sensing of the ocean and computation fluid dynamics.

CUIHONG PAN was born in Guangdong, China, in 1993. She received the B.S. degree from Guangzhou University, in 2017, where she is currently pursuing the M.S. degree. Her major is in geographical information science. Her research interest includes ocean remote sensing and applications.

HAITAO LI was born in Guangdong, China, in 1996. She received the B.S. degree from Guangzhou University, in 2019, where she is currently pursuing the M.S. degree. Her major is geographical information science. Her research interests include ocean remote sensing and big data applications.